

Influence of Grinding Parameters on Strength-Dominating Near-Surface Characteristics of Silicon Nitride Ceramics

W. Pfeiffer & T. Hollstein

Fraunhofer-Institut für Werkstoffmechanik (IWM), D-79108 Freiburg, Germany

(Received 15 September 1995; accepted 10 June 1996)

Abstract

The complex relationship between machining parameters, surface quality and strength of sintered silicon nitride (SSN) was investigated using roughness measurements, SEM observations, strength tests and X-ray diffraction techniques. Conventional grinding as well as creep-feed grinding, high-speed grinding and grinding at high material removal rates have been studied. From the results detailed information is derived about the effect of different grinding parameters on near-surface effects and on strength. The results demonstrate the limitations of often proposed correlations between strength and other 'characteristics' of machined surfaces, like roughness values or theoretically derived values of the chip thickness. Guidelines for optimized grinding parameters are established. © 1996 Elsevier Science Limited.

Die komplexen Zusammenhänge zwischen Bearbeitungsparametern, Oberflächenqualität und Festigkeit von drucklos gesintertem Siliciumnitrid (SSN) wurden mit Hilfe von Rauheitsmessungen, REM-Untersuchungen, Festigkeitsermittlungen und röntgenographischen Beugungsanalysen untersucht. Berücksichtigt wurden die Bearbeitungsvarianten Pendelschleifen, Tiefschleifen, Hochgeschwindigkeitsschleifen und Schleifen mit hohen Abtragsleistungen. Aus den Ergebnissen werden detaillierte Informationen über den Einfluß der verschiedenen Bearbeitungsparameter auf den Randschichtzustand und auf die Festigkeit gewonnen. Die Ergebnisse zeigen auch die Grenzen für oft postulierte Zusammenhänge zwischen Festigkeit und anderen Charakteristika bearbeiteter Randschichten, wie z.B. Rauheit oder

theoretisch abgeleiteten Spannungsdicken an der Einzelschneide, auf. Es werden Richtlinien für optimierte Bearbeitungsparameter angegeben.

1 Introduction

The high quality required for components of structural ceramics can often be achieved only by an additionally applied machining process. Machining can strongly influence the strength and service behaviour of the components, and, in addition, represents a considerable part of the manufacturing costs. Therefore machining should be optimized not only according to economical aspects, but it must also be guaranteed that the surface layer damage does not exceed permissible limits.

The quantification of machining damage on the basis of characteristics that can be determined simply (e.g. roughness parameters) may lead to a wrong assessment of strength properties.¹ Thus, for example, silicon nitride samples lapped with coarse-grained abrasives can show higher strengths than polished ones.² High-resolution analysis methods (e.g. acoustic or thermal microscopy) often fail to detect machining damage efficiently because of the conflicting demands for the examination of large areas at a high local resolution for the detection of (often only a few μm large) flaws, which may cause fracture. Additionally, sometimes the component does not fail at the largest flaw detected. All these non-destructive methods are therefore less suitable for a determination of strength-relevant surface layer properties.

X-ray diffraction methods offer the possibility of an accurate assessment of machining quality.^{1,3} These methods quantify machining-induced damage by determining the amount of machining-induced

residual stresses and microplastic deformation of the surface layer.

2 Experimental Procedures

2.1 Materials and machining

The material investigated was a commercial sintered silicon nitride (SN-N3204 from Cremer Forschungs-Institut, CFI). Four-point bend specimens (45 mm × 4 mm × 3 mm) were ground in the longitudinal and transverse directions. Two different diamond wheels were used (both with a 126 μm grit size): a resin-bonded wheel type D126K + 1313 RYB C75 and a D126 HP700 wheel (electrochemically bonded monolayer of diamonds). Up-cut surface grinding was performed at different infeeds ($0.15 \text{ mm} \leq a_c \leq 3.5 \text{ mm}$), specific material removal rates [$5 \text{ mm}^3/(\text{mm s}) \leq Q'_w \leq 25 \text{ mm}^3/(\text{mm s})$] and grinding speeds ($30 \text{ m s}^{-1} \leq V_c \leq 150 \text{ m s}^{-1}$). As coolant, Petrofer Isocut R118 grinding oil was supplied by a single high-pressure jet.

2.2 Characterisation of near-surface conditions and strength

The near-surface conditions of the samples were characterized by conventional roughness measurements, strength tests and X-ray diffraction methods.

The roughness measurements were conducted using a surface profilometer with a stylus of 5 μm radius tip. Average roughness values R_a and average peak-to-valley heights $R_{z,DIN}$ were determined transverse to the grinding direction.

The strengths of the machined surface layers were determined using four-point bend tests following the DIN standard.⁴ The characteristic bending strengths σ_0 and the Weibull moduli m were evaluated from the fracture stresses of up to 20 samples with identically machined surfaces. The 90% confidence ranges of σ_0 and m were calculated using the Monte-Carlo simulation.⁵ Owing to the small number of samples within several series the uncertainties of calculated Weibull moduli are large, and differences between the different grinding conditions are therefore not discussed.

Strength-relevant machining-induced near-surface effects, i.e. damage and residual stresses, were assessed by X-ray diffraction analyses. Because of the small penetration depth of the X-rays used in diffraction experiments, machining-induced residual stresses can be determined directly by X-ray stress analysis. The amount of damage is evaluated in an indirect way by measurement of the amount of microplastic deformation (dislocation density). It has previously been shown that the micromechanical loading conditions of the material during machin-

ing and therefore the degree of damage of the machined surface can be quantified by the amount of microplastic deformation. The X-ray diffraction methods inspect relatively large areas. This takes the statistical meaning of 'damage' into account and avoids a time-consuming search for microscopic small cracks. In most cases for machined ceramics the strength-decreasing damage prevails against the strength-increasing compressive residual stresses.⁷ Thus, from the amount of the microplastic deformation, the strength of the surface layer can often be assessed.

Average values of microplastic deformation and residual stresses were determined over the effective penetration depth of X-rays (8 μm). In some cases, the depth distributions within the first 30 μm were also evaluated. Details of the methods used are described elsewhere.^{2,3}

2.3 Assessment of the effect of damage and residual stresses on strength

The effect of machining-induced residual stresses and damage on the strength is evaluated by means of fracture mechanics calculation from the bending strength data σ_0 and the experimentally determined residual stress distributions $\sigma_{RS}(z)$ according to eqns (1) and (2). The calculated 'flaw sizes' a_c are, of course, affected by the simplifications used but nevertheless they characterize the amount of damage. Ideal, sharp, scratch-like surface cracks were assumed ($f = 1.12$) in case of transverse ground bend bars and the appropriate value of fracture toughness K_{Ic} for small cracks ($3.5 \text{ MPa } \sqrt{\text{m}}^{1/2}$) was used. Details of this fracture mechanically based evaluation method are given elsewhere.^{2,6}

$$K_{Ic} = \sigma_c f \sqrt{\pi a_c}$$

with

$$\sigma_c = [\sigma_0(z) + \sigma_{RS}(z)]$$

where z = distance from sample surface.

2.4 Assessment of elementary grinding mechanisms

The elementary grinding conditions at the individual grits of the grinding wheel were characterized by calculated values of the mean chip thickness at the single cutting edges. Calculation was performed following the method of Werner⁸ by setting the 'internal' material removal rate equal to the 'external' material removal rate. The 'internal' removal rate is given by grinding wheel characteristics, i.e. the number of active grits and the grit size, by the contact length between wheel and sample, by the cutting speed v_c and by the chip thickness at the individual grit, h_{cu} . The 'external' removal rate is given by the infeed a_c and by the tangential feed rate v_{ft} . It must be pointed out that these values of

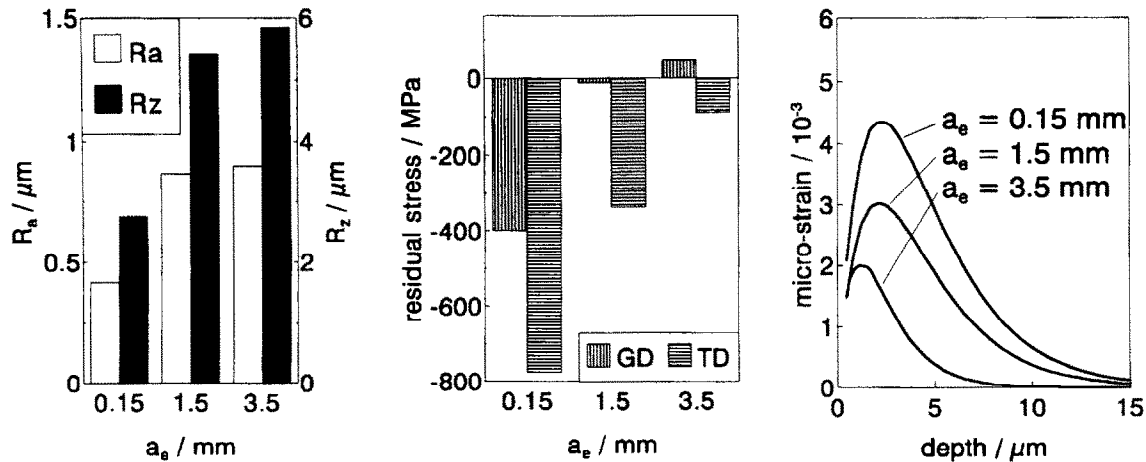


Fig. 1. Influence of the infeed a_e on roughness values, average values of near-surface residual stresses and depth distributions of microplastic deformation of ground samples. ($Q_w = 15 \text{ mm}^3/(\text{mm s})$, $v_c = 30 \text{ m/s}^{-1}$, TD = residual stress in transverse direction, GD = residual stress in grinding direction).

calculated chip thickness can be at best rough estimations of elementary grinding conditions, since wear or splitting of grits (for example) is not taken into account.

3 Results and Discussion

3.1 Effect of machining parameters on near-surface conditions and strength

Figure 1 shows the influence of the infeed (depth of cut) for grinding at a constant specific material removal rate of $15 \text{ mm}^3/(\text{mm s})$ and $v_c = 30 \text{ m s}^{-1}$. Changing the grinding conditions from conventional conditions ($a_e = 0.15 \text{ mm}$) to creep feed ($a_e = 3.5 \text{ mm}$) the depth of cut at the individual grits — and by this roughness and damage — is commonly assumed to decrease.

The values determined for R_a and R_z indicate the opposite effect, both values being increased for creep-feed grinding. Scanning electron micrographs (Fig. 2) show large amounts of macroplastic deformation at the conventional ground surface. This visual impression suggests that the conven-

tional grinding operation has smeared material into the grinding grooves, reducing the roughness of the surface. This conjecture is confirmed by the microstrain and residual stress states shown in Fig. 1.

Large compressive residual stresses are created, especially transverse to the grinding direction for low infeeds. The strong dependency of residual stresses on the grinding direction is in agreement with the assumption of a significant contribution of macroscopic plastic deformation in the surface region after conventional grinding. The depth distributions of microstrain (Fig. 1) show the machining-induced microplastic deformation of the near-surface regions. Both the amount and depth of microplastic deformation are increased from creep-feed grinding conditions to conventional grinding conditions.

Both results, the increase of compressive residual stresses and microplastic deformations for conventional grinding conditions, bear out the expected increase of the grinding forces at the individual grits. Thus, relatively high damage can be expected in the case of conventional grinding.

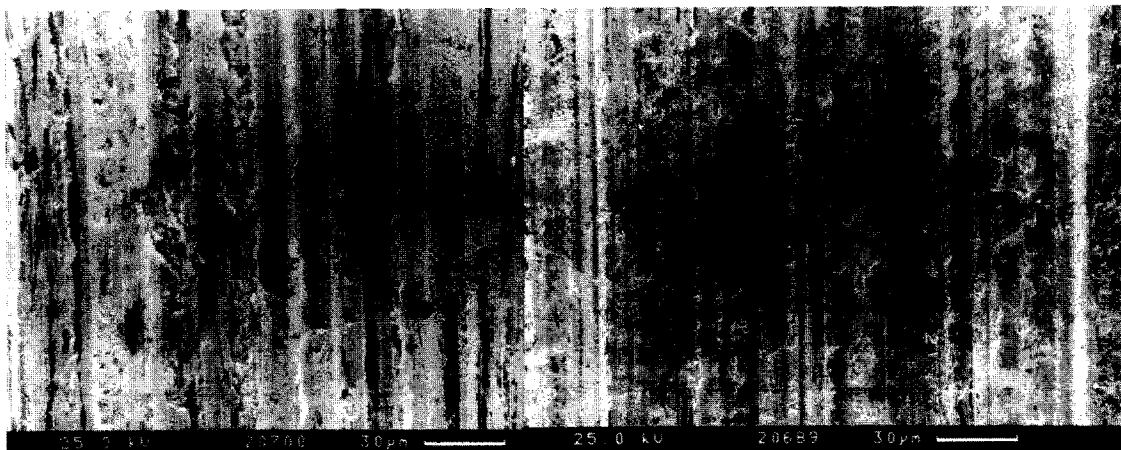


Fig. 2. SEM micrographs of ground silicon nitride. Left: conventional grinding ($a_e = 0.15 \text{ mm}$), average roughness $R_a = 0.42 \text{ }\mu\text{m}$. Right: creep-feed grinding ($a_e = 3.5 \text{ mm}$), average roughness $R_a = 0.90 \text{ }\mu\text{m}$.

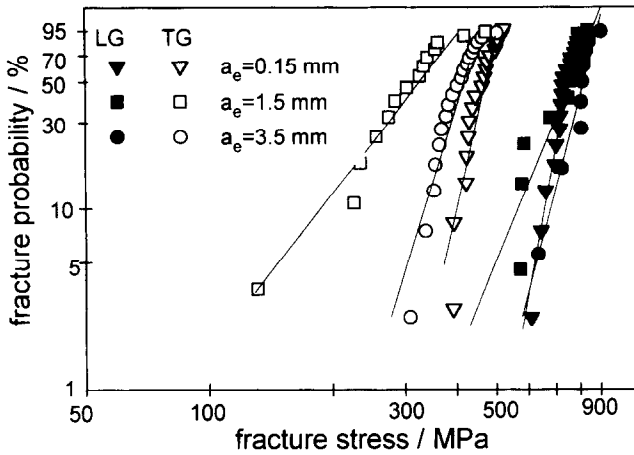


Fig. 3. Influence of the infeed a_e on the Weibull distributions of fracture stresses of samples ground in longitudinal and transverse directions. ($Q'_w = 15 \text{ mm}^3/(\text{mm s})$, $v_c = 30 \text{ m s}^{-1}$, LG = longitudinally ground, TG = transversely ground.)

The Weibull distributions of bending strengths of the differently ground samples are shown in Figs 3 and 4. As often obtained⁹ and as indicated from the strong direction dependency of the residual stresses, the bending strength of longitudinally ground samples is substantially higher than the strength of transverse ground samples. There is no clear tendency of the influence of the infeed on strength. In the case of the longitudinally ground samples no significant difference exists between the characteristic bending strength data of the differently ground samples (Fig. 4, left). The effect of strength-increasing compressive residual stresses is negligible (see Fig. 1). In case of the transverse ground samples (Fig. 4, right) the opposite effects of compressive residual stresses and damage may be the reason for the unexpected result.

To clarify this situation, the strength-relevant effects of grinding-induced residual stresses and damage were quantified by flaw sizes a_c and critical fracture stresses σ_c calculated according to eqns (1) and (2). In Fig. 5, left the depths of such 'flaws' calculated with the effect of residual

stresses included, are shown. These 'flaws' represent the actual machining-induced damage. From these calculations it can be concluded that grinding with the highest infeed ($a_e = 3.5 \text{ mm}$) induces only shallow flaws parallel to grinding direction, whereas deeper flaws are induced with smaller inffeeds.

The comparison of the bending strengths and the calculated fracture stresses (Fig. 5, right) shows clearly the significant contribution of compressive residual stresses to the strengths of the transverse ground samples. The largest contribution of machining-induced residual stresses is evaluated for the conventionally ground samples ($a_e = 0.15 \text{ mm}$). Due to the high compressive residual stresses these samples exhibit the best transverse bending strength although relatively large flaws were generated. The grinding conditions with medium and large inffeeds cause deeper flaws or less strength-increasing residual stresses, respectively, leading to lower bending strengths than the conventionally ground samples.

The influence of increased specific material removal rates (Q'_w) for longitudinal creep-feed grinding ($a_e = 1.5 \text{ mm}$, $v_c = 30 \text{ m s}^{-1}$) is shown in Fig. 6. Increasing the specific material removal rate by increasing the tangential feed rate increases the depth of cut at the individual grits and consequently the roughness and damage. Here the determined values of R_a and R_z are in agreement with the expected effect of the grinding parameters. Significant compressive residual stresses are again created transverse to the grinding direction, whereas parallel to the grinding direction almost no residual stresses are present. The highest near-surface influence is evaluated for the medium specific material removal rate of $15 \text{ mm}^3/(\text{mm s})$: both compressive residual stresses and depth of microplastic deformation are highest. Only very near the surface the high material removal rate induced the highest deformation.

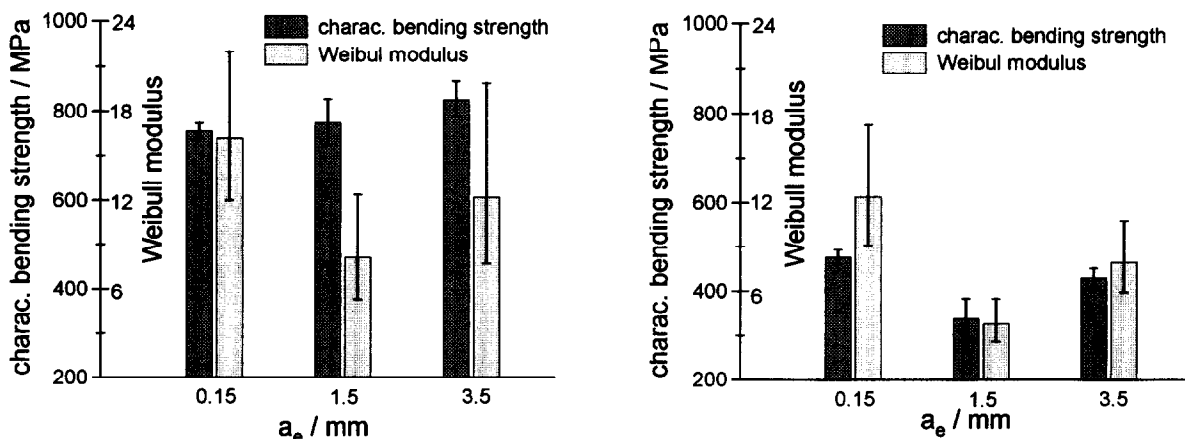


Fig. 4. Influence of the infeed a_e on the characteristic bending strengths and Weibull moduli of samples ground in longitudinal (left) and transverse (right) directions ($Q'_w = 15 \text{ mm}^3/(\text{mm s})$, $v_c = 30 \text{ m s}^{-1}$).

The strength data of the longitudinal ground samples are shown in Fig. 7. As expected, the best bending strengths are obtained with samples ground with the smallest material removal rate. The lowest strength is obtained with samples

ground with a medium material removal rate. This is in agreement with the residual stress and microdeformation states (see Fig. 6) but it is not expected from theoretical considerations about the grit depth of cut. Since no significant compressive

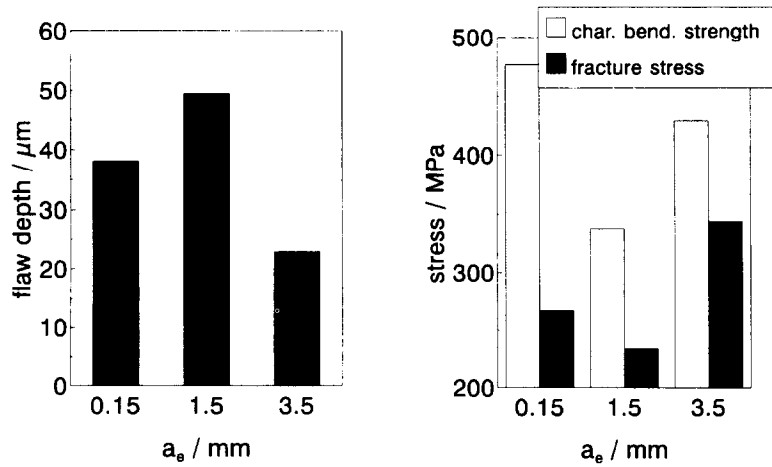


Fig. 5. Depths of fracture causing flaws of transversally ground samples, calculated with the effect of residual stresses included (left), and characteristic bending strengths compared with calculated actual fracture stresses which take into account the residual stress effects (right).

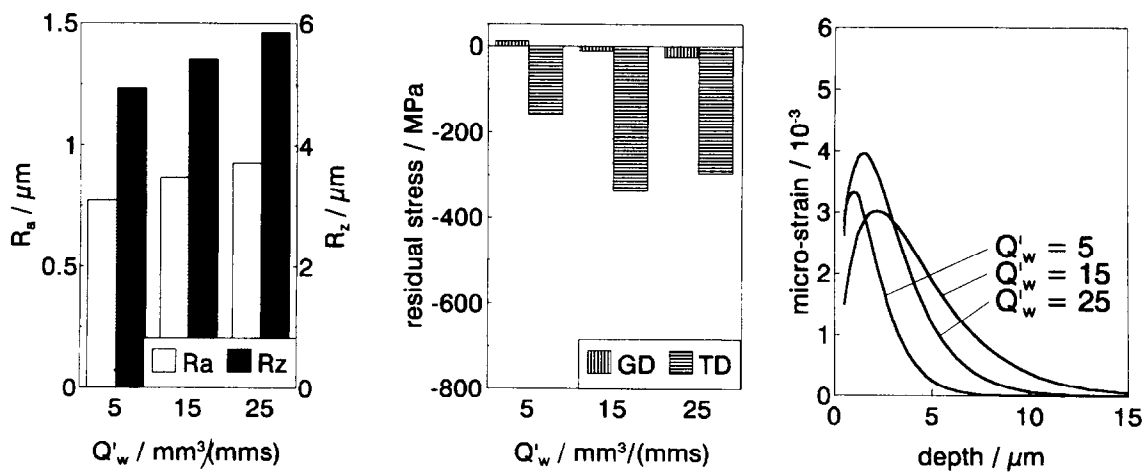


Fig. 6. Influence of the specific material removal rate Q'_w on roughness values, average values of near-surface residual stresses and depth distributions of microplastic deformation of ground samples. ($a_e = 1.5$ mm, $v_c = 30$ m s⁻¹, TD = residual stress in transverse direction, GD = residual stress in grinding direction.)

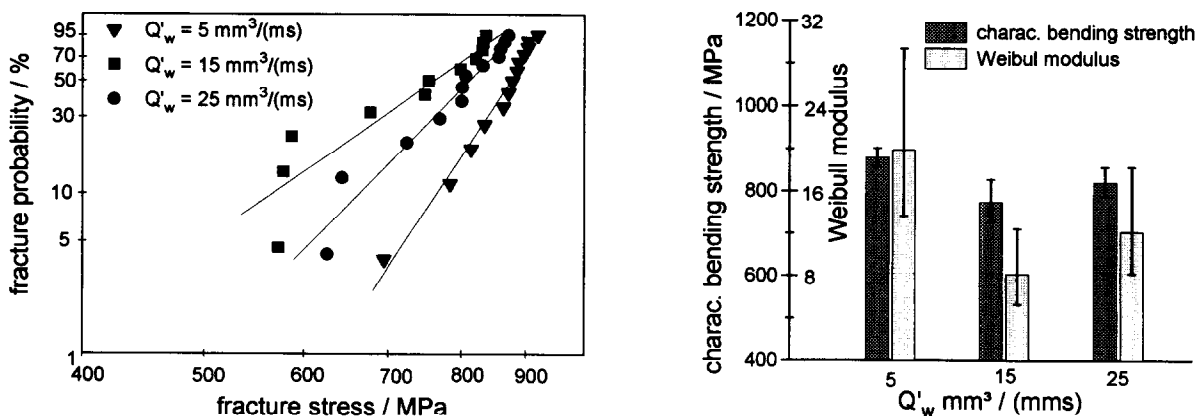


Fig. 7. Influence of the specific material removal rate Q'_w on Weibull distributions of fracture stress (left) and characteristic bending strengths and Weibull moduli (right) of longitudinally ground samples ($a_e = 1.5$ mm, $v_c = 30$ m s⁻¹).

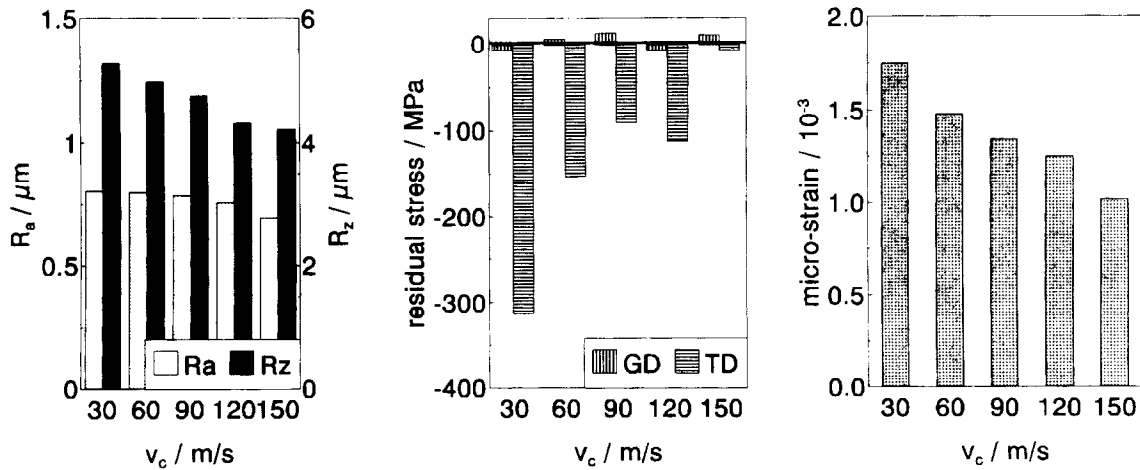


Fig. 8. Influence of the cutting speed v_c on roughness values, average values of near-surface residual stresses and microplastic deformation of longitudinally ground samples. ($Q'_w = 5 \text{ mm}^3/(\text{mm s})$, $a_c = 1 \text{ mm}$, TD = residual stress in transverse direction, GD = residual stress in grinding direction.)

residual stresses exist parallel to the grinding direction it can be concluded, again, that bending strength of longitudinally ground samples is dominated by damage.

The dependency of the surface roughness, the near-surface residual stress and the microplastic deformation on the cutting speed v_c is shown in Fig. 8. A special monolayered diamond wheel was used for these grinding experiments. All samples were longitudinally creep-feed ground ($a_c = 1 \text{ mm}$) at a 'moderate' constant specific material removal rate of $5 \text{ mm}^3/(\text{mm s})$. Increasing the cutting speed leads to a reduced depth of cut at the individual grits due to a larger number of simultaneously acting grits. Thus, roughness, residual stresses and damage are expected to decrease too.

The decreasing residual stresses and microplastic deformations show, indeed, that the micro-mechanical loading of the near-surface regions can be reduced by grinding with increased cutting speeds. The samples ground at the maximum cut-

ting speed no longer show significant residual stresses and the microstrain state has reached the low level of the bulk material. Additionally, the 'surface quality', characterized by the roughness values R_a and R_z , is best at high cutting speeds. Therefore a decrease of damage and possibly an increase of strength can be expected for samples ground with high cutting speeds.

The Weibull distributions of fracture stresses and the characteristic bending strengths of these specimens are shown in Figs 9 and 10. The expected effect of the cutting speed on strength is very small within the longitudinally and transverse ground series. Due to the limited amount of available material the strength distributions could not be determined for all cutting speeds. As indicated by the negligible residual stress components parallel to the grinding direction, the effect of machining-induced damage on strength of the longitudinally ground samples is negligible. Bending strength is at the level of the bulk material and no further increase due to increased cutting speeds can be expected.

In the case of the transversely ground samples, again the opposite effects of compressive residual stresses and damage seem to be the reason for the small influence of the grinding parameters on strength.

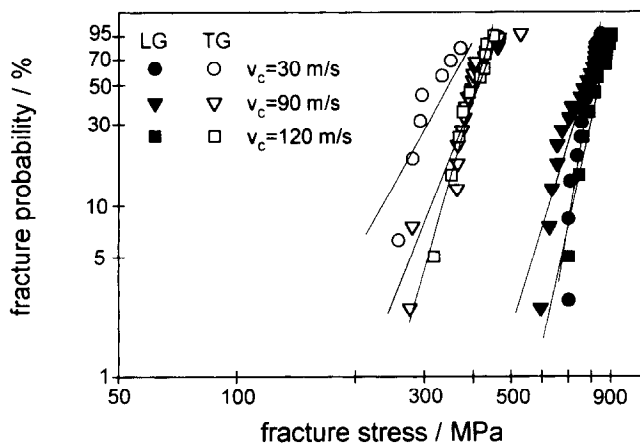


Fig. 9. Influence of the cutting speed v_c on the Weibull distributions of the fracture stresses of the samples ground in longitudinal and transverse directions ($Q'_w = 5 \text{ mm}^3/(\text{mm s})$, $a_c = 1 \text{ mm}$, LG = longitudinally ground, TG = transverse ground).

3.2 Correlations between near-surface characteristics and calculated chip thicknesses

The results shown above indicate that only the machining-induced residual stresses and the microplastic deformation can be expected to correlate with elementary characteristics of the material removal mechanisms. Near-surface characteristics like strength are possibly the result of the opposite effects of damage and residual stresses, and they may therefore be less suitable to characterize the

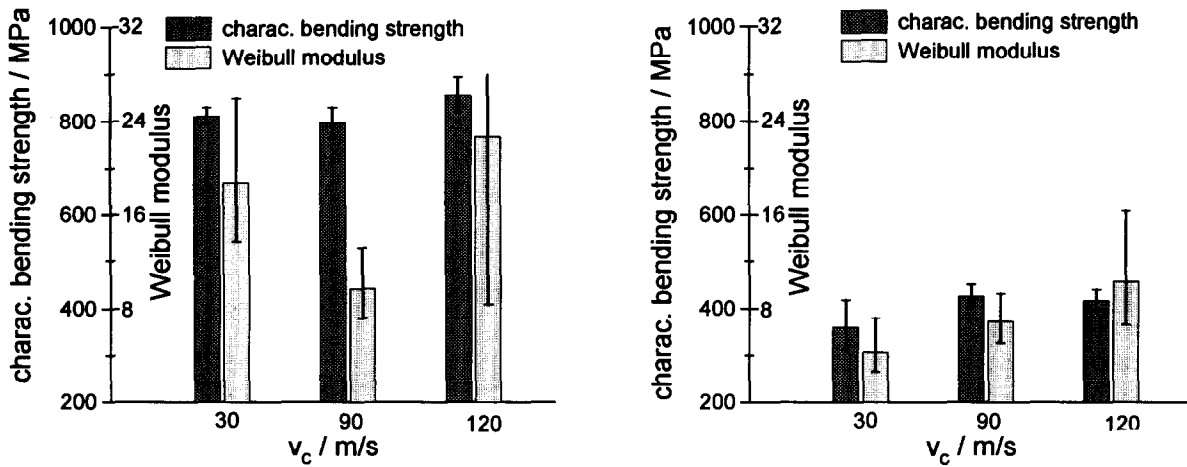


Fig. 10. Influence of the cutting speed v_c on characteristic bending strengths and Weibull moduli of samples ground in longitudinal (left) and transverse (right) directions ($Q_w = 5 \text{ mm}^3/(\text{mm s})$, $a_c = 1 \text{ mm}$).

material removal process. Thus, the average residual stresses of the near-surface layers of differently ground samples were plotted versus the mean chip thickness at the individual cutting edges, h_{cu} (grit depth of cut).

Figure 11 shows the results obtained from samples ground with a conventional D126K+ grinding wheel and with a wheel with a monolayer of diamonds (D126HP700). The results obtained from the samples ground with the conventional wheel (Fig. 11, right) show the limitations of an assessment of the material removal mechanisms on the basis of the grit depth of cut, which is calculated from the grinding parameters. The residual stresses after machining using a wider range of grinding parameters exhibit no clear dependence on the chip thickness. Obviously some important effects of the real material removal process, e.g. blunting or chipping of the diamonds, are of significant influence on the resulting near-surface conditions but they are not considered in the calculated grit depth of cut. If more 'easily' describable grinding wheels (e.g. with a monolayer deposit of diamonds)

are used and only limited variations of grinding parameters are applied (e.g. cutting speed), the expected influence of decreasing chip thicknesses on the amount of near-surface residual stresses is qualitatively confirmed (Fig. 11, left).

4 Conclusions

The near-surface conditions of differently ground silicon nitride samples were characterized by conventional roughness measurements, strength tests and X-ray diffraction methods.

The strength tests show that a low surface roughness in some cases is not correlated with a high strength. Strength-controlling near-surface effects were therefore characterized by the amount of machining-induced residual stresses and microplastic deformation. Residual stresses and microplastic deformation are direct measurable parameters of the locally acting forces during machining, and they can be determined non-destructively by X-ray diffraction methods.

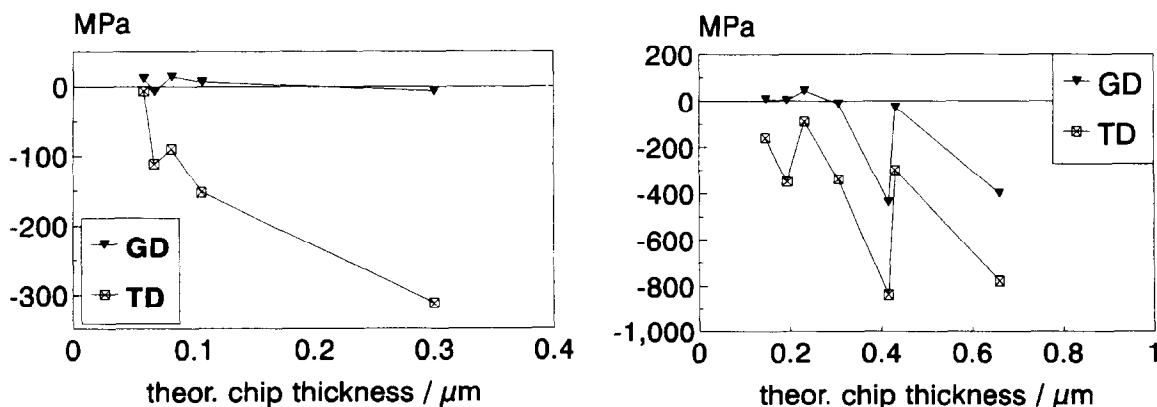


Fig. 11. Machining-induced residual stresses versus theoretically calculated values of chip thickness. Left: Monolayer grinding wheel, variation of grinding speed, $Q_w = 15 \text{ mm}^3/(\text{mm s})$. Right: Conventional grinding wheel, variation of grinding speed, infeed and tangential feed rate.

Significant compressive residual stresses are in most cases created only transverse to the grinding direction, indicating an extremely preferred orientation of the micromechanical loading during grinding. This is confirmed by the bending strength of longitudinally ground samples, which are substantially higher than the strengths of transversely ground samples.

No significant influence of the infeed and cutting speed and only little influence of the material removal rate on the strengths of longitudinally ground samples can be observed. Fracture mechanically based calculations show that, for transversely ground samples, the high compressive residual stresses overcompensate the damage if small infeeds are used. Thus the best bending strengths of transversely ground samples are achieved with conventional grinding conditions. Similar mechanisms are responsible for the negligible dependency of the bending strength on the cutting speed.

Only rough estimations about damage effects are possible on the basis of the calculated values of the grit depth of cut. Due to uncertainties concerning the cutting conditions at the active individual grits and due to the opposite effects of machining-induced damage and residual stresses on strength, in certain cases one can be led to a wrong assessment of strength properties.

Acknowledgements

Grinding of the samples was performed by J. Wimmer and M. Zapp, University of Kaiserslautern (FBK), Germany. The material was

supplied by the Cremer Forschungsinstitut GmbH, Rödental, Germany. Part of the investigations was sponsored by the Bundesministerium für Forschung und Technologie (BMFT), and by a consortium of industrial companies within the project 'Schleifen von Hochleistungskeramik'.

References

- Hollstein, T., Pfeiffer, W., Schinker, M., Thielicke, B. & Voß, B.: Bauteilprüfung und Qualitätssicherung. In: *Schleifen von Hochleistungskeramik*. Verlag TÜV Rheinland, Köln, 1994, pp. 197–232.
- Pfeiffer, W. & Sommer, E.: Bewertung der Festigkeitseigenschaften oberflächenbearbeiteter Keramikbauteile. In *Werkstoffkunde*. DGM Informationsgesellschaft mbH, Oberursel, 1991, pp. 575–584.
- Pfeiffer, W. & Hollstein, T.: Damage determination and strength prediction of machined ceramics by X-ray diffraction techniques. In *Machining of Advanced Materials*. NIST Special Publication 847, United States Department of Commerce 1993, pp. 235–245.
- DIN 51 110, Teil 1: Prüfung von keramischen Hochleistungswerkstoffen. 4-Punkt-Biegeversuch bei Raumtemperatur.
- Thoman, D. R., Bain, L. J. & Antle, C. E.: Inferences on the parameters of the Weibull distribution. *Technometrics*, **11** (1969) 445–460.
- Pfeiffer, W., Hollstein, T. & Sommer, E.: Strength properties of surface-machined components of structural ceramics. In *Fracture Mechanics*, 25th Vol., ASTM STP 1220. American Society for Testing and Materials, Philadelphia, USA, 1994.
- Pfeiffer, W. & Hollstein, T.: Einfluß einer Endbearbeitung auf das Festigkeitsverhalten und den Oberflächenzustand. *Fortschrittsberichte der Deutschen Keramischen Gesellschaft*, **7** (1992) 55–63.
- Werner, G.: Kinematik und Mechanik des Schleifprozesses. Dissertation, Th. Aachen, 1971.
- Rice, R. W.: Effects of ceramic microstructural character on machining direction-strength anisotropy. In *Machining of Advanced Materials*. NIST Special Publication 847, United States Department of Commerce, 1993, pp. 185–204.